ASSESSING THE EFFECT OF MECHANICAL DEFORMATION OF THE PANASONIC NCR18650B LITHIUM-ION POWER CELL HOUSING ON ITS FIRE SAFETY

This paper considers the deformation properties of the body of the lithium-ion power cell (LIPC) Panasonic NCR18650B ($LiNi_{0.8}Co_{0.15}Al_{0.05}O_2$) exposed to the action of static load at various techniques of fixing the cell. Determining the properties of LIPCs under appropriate conditions makes it possible to fill the gap in existing studies, which will further ensure the safety of their use.

Based on the results of experimental studies, the LIPC rigidity and temperature indicators were determined in accordance with the applied load. The most dangerous variant, from the point of view of fire danger, of applying a static load on the cell has been established.

It was experimentally established that, on average, the Panasonic NCR18650B LIPC housing can withstand a load of about 80 kg·s/cm² (or 7.84 MPa) without further ignition. An increase in pressure force in the range exceeding 85–90 kg·s/cm² leads to an irreversible chain thermochemical reaction, which, within 2–3 seconds, leads to LIPC ignition. Compressing the LIPC evenly along its lateral surface showed the occurrence of combustion at the load on the cell equal to 150 kg·s/cm². The average temperature of the cell during combustion caused by the deformation of the housing is 350–450 °C, and the maximum value is registered in the range of 580–680 °C.

The mathematical model built on the basis of the mathematical theory of thin shells adequately describes the stressed-strained state of the cylindrical body of cells under the action of a force concentrated and distributed load. The estimation model is satisfactorily verified by experimental results, making it possible to improve the strength and rigidity of LIPC housing by choosing the appropriate steel grade for its body, the geometric dimensions, and the structural technique of its fastening

Keywords: Panasonic NCR18650B, mechanical deformation, combustion temperature, mathematical model, fire hazard

Oleksandr Lazarenko
Corresponding author
PhD, Associate Professor*
E-mail: o.lazarenko@ldubgd.edu.ua
Taras Hembara
PhD, Associate Professor
Department of Applied Mathematics and Mechanics**
Vitalii Pospolitak
Department of Vocational Training**
Dmytro Voytovych
PhD, Associate Professor*
*Department of Fire Tactics and Emergency Rescue Operations**
**Lviv State University of Life Safety
Kleparivska str., 35, Lviv, Ukraine, 79007

1. Introduction

Modern heavy-duty batteries are not typical lead-acid products with a voltage of 12–24 V and above. In the overwhelming majority, rechargable batteries consisting of a large number of lithium-ion power cells (LIPCs) of various formats (sizes), capacities, chemical composition, etc. are becoming increasingly popular and practical. Due to their advantages, rechargable batteries, namely LIPCs, have become widely used in modern electric vehicles, various power tools and household appliances. A striking example of the modern application of LIPC as rechargable batteries is the production and ever-growing demand for cars such as Tesla, Nissan Leaf, Chevrolet Bolt (Volt), and many others.

Safe and reliable operation is a key and main indicator of LIPC efficiency. The safe working conditions of LIPC are largely determined by the chemical composition of the cells [1, 2], the working environment of operation, and resistance to external factors, among which emergency power loads on the housing are especially dangerous. Also, during daily operation, LIPC may intentionally or accidentally experience cases of operation at elevated currents [3], mechanical damage [4], elevated external temperatures. Under such conditions, this can lead to the burning of LIPC or even an explosion [5]. One of the determining factors of LIPC fire safety, in particular for an electric car, is the stability of a geometric shape, that is, the rigidity of the LIPC body. As a rule, LIPC housings serve as a protective layer aimed at withstanding external mechanical stress and maintaining the electrochemical integrity of the internal environment of the cell.

To analyze the boundary working conditions of various types of LIPC, safety standards have been developed and appropriate tests to determine the productivity of their work are aimed at meeting the necessary safety requirements. For example, there are a number of national and international standards in countries such as the United States, China [6, 7], and others, thus they help implement strict standards for the safe operation of LIPC produced and used. Such tests are aimed at the safety of LIPC and conditionally guarantee the absence of future problems with the safety of LIPC under normal conditions of their use.

Therefore, the creation of a scientifically based basis for determining the techniques and means for mechanical protection of vulnerable technical cells in various equipment predetermines our research. Thus, taking into account the mechanism of electrochemical reactions, the mechanical behavior of the LIPC shell material, the properties of materials and adverse reactions occurring in LIPC is fundamental for assessing their fire safety.

2. Literature review and problem statement

Earlier studies into determining the fire hazard of LIPC Panasonic NCR18650B as a result of its mechanical damage (due to piercing it with a sharp object) and the action of excessive current [3, 4] show a relatively similar result. Given the variety of probabilistic ways for disrupting the stable conditions of LIPC functioning, the issue of LIPC fire danger resulting from the action of mechanical deformation of the cell housing remains unresolved.

Considering the scientific findings regarding the effect of deformation (compression) of LIPC, it can be argued that in this area authors are limited to the following conclusions:

– taking into account the statistical indicators of ignition of lithium-ion power cells due to mechanical deformation, the authors of work [8] focused their attention on the study of the deformation rate of LIPC 18650 NCA. The paper reports experimental studies on deformation of a LIPC housing at different load speeds of 1, 5, and 10 mm/min. Taking into account experimental studies, a finite-element model of the stressed-strained state of the modular cell holder was built and tested. The analytical and experimental results are the basis for the development and further study of the strength and protective properties of a special LIPC modular holder. It was found that the presence of a modular holder effectively improves the distribution of the high-pressure area under shock load but causes a dangerous local increase in compression stresses. Among the factors affecting the failure of the battery, the speed of the object facing the obstacle, that is, dynamic characteristics, is decisive;

– in study [9], the authors solved a complex analytical and theoretical problem of studying the parameters that control the flat deformation of the power cell. Some analytical approaches are used in the work, as well as computational models of a representative volume cell (RVE). The resulting estimation models were tested on the basis of experiments; the effectiveness of the proposed approach was shown, which provides a tool for modeling battery failures and designing effective protective structural cells for LIPC. The importance of the proposed method is the fact that the analytical and RVE models give an idea of the influence of both geometric anisotropic and material properties of the constituent inner layers on the level of the stressed-strained state of the cell.

As a limitation of that study, it should be noted that the proposed method is applicable only to flat sections of prismatic and package LIPCs and cannot be fully applied to cylindrical LIPCs;

– important theoretical and experimental results are reported in [10], where researchers conducted a comprehensive study of the effect of mechanical deformation of prismatic LIPC on its mechanical properties. The authors conducted a number of quasistatic and dynamic experiments aimed at compressing LIPC at different speeds and degrees of LIPC charge. The experiments were primarily aimed at obtaining indicators of critical displacement of the inner layers of the prismatic LIPC. The experimental results made it possible to simulate the process under study on the Ls-Dyna computing platform and further compare it with experimental data. Based on the results of the research, the criteria for destruction were established as critically permissible deformations, or compression stresses, depending on the level of battery charge, which is of particular practical interest.

Based on the results of the research, the criterion of destruction was established, which is determined by the extrusion displacement of the cell of the prismatic lithium-ion power cell; the corresponding critical pressure of destruction is 5.652 MPa:

– unlike many similar studies, the authors in work [11] focused their attention on the study of parameters of the material for a shell of the cylindrical LIPC. A detailed study into the properties of the LIPC shell during exposure to external load, according to the researchers, plays a key role in ensuring the rigidity of the lithium-ion power cell body under external compressive load. The experimental studies involved the outer shells of commercial LIPC 18650 NCA (nickel-cobalt-aluminum-oxide). Under laboratory conditions, the dynamic behavior of LIPC shell material was investigated.

Based on the results of the research, both theoretical constitutive analytical and numerical models were developed that can describe the mechanical behavior of the battery shell material under shock load. It was first revealed that given the effect of the deformation rate of the shell material, increasing the strength of the shell material may even contribute to the occurrence of a short circuit in LIPC. In general, the results of that scientific work lay a scientific precaution regarding the safety of the LIPC structure as a whole in the context of the choice of the material of the body of cylindrical LIPC;

– an addition to the results of work [11] is the scientific results reported in article [12]. The researchers, based on the obtained experimental values of the degree of deformation of the cylindrical LIPC, constructed a mathematical model for a detailed analysis of the deformation reaction of LIPC to the load. Using the resulting analysis and mathematical apparatus, a description of the LLIPC deformation reaction to the applied load was prepared, subject to static load, where factors such as correlation of housing deformation and the degree of LIPC charge were taken into account. In the end, a satisfactory comparison of the obtained experimental values with the calculated ones according to the mathematical model is carried out, which makes it possible, in the opinion of the authors, to conduct a study into the LIPC parameters under the dynamic load;

– scientific results of work [13] is the determination of mechanical-electrical-thermal reactions of prismatic LIPC of large capacity, subject to the action of quasistatic and dynamic mechanical load. For a detailed study of the degree of deformation of the LIPC, and especially the degree of displacement of the inner wrapper (cathode-anode-separator) of the LIPC, the authors used a high-resolution X-ray machine. Based on the results of the work, clear thermal reactions were investigated depending on the applied load directions. For example, the surface temperature of a fully discharged LIPC under the deformation site quickly rose by 70 °C after a voltage drop;

– from the point of fire danger, the scientific results of research are reported in [14]. The authors tried to investi-

gate the fire hazard indicators of cylindrical LIPC of various formats and chemical composition (LFP, NCA) depending on the mechanical damage to the LIPC. For research, two types of mechanical damage to the LIPC were chosen – penetration of the housing with a sharp object and deformation of the LIPC under pressure. In general, based on the results of research, it was found that due to mechanical damage, intensive combustion of LIPC occurs with intensive release of sparks and heat; the total temperature indicators fluctuate in the range of 122–812 °C;

– the actual continuation and addition to works [11, 12] are the scientific results reported in study [15]. Theoretical and experimental research in the work was divided into several stages. During the first stage, the dynamic characteristics and parameters of the cylindrical LIPC material (outer steel shell, cathode, anode) for tensile (deformation rate) were experimentally and theoretically investigated. After that, a numerical mathematical model of the process under study was developed and an experimental study was carried out to determine the degree of deformation of the LIPC, subject to a dynamic load on it. A valid 3D model of the deformation behavior of the cylindrical LIPC, format 18650, was also developed, subject to the influence of external load;

– in [16], there is a systematic approach to modeling progressive failures and predicting short circuits directly in the cathode-separator-anode environment. The paper experimentally investigated the deformation and progressive behavior of the internal components of LIPC. In particular, a sample (cathode-separator-anode) consisting of five layers was selected for the study, under conditions of static deformation. Based on the results of experimental research, three different mathematical models were built, namely, a detailed model of high accuracy, an intermediate homogenized model, and a fully homogenized model. The authors showed that the resulting mathematical models can be used with varying degrees of accuracy to simulate the progressive failure of a multilayer battery sample.

Analyzing the results of scientific research aimed at identifying patterns and phenomena arising in LIPC as a result of its deformation, we can unequivocally state the following:

– the issue of fire danger of the LIPC itself was not a sufficiently thorough subject of consideration of the work;

– determination of the temperature indicators of the cell was carried out within 100 °C.

Only in [14] the authors tried to outline the main temperature indicators of LIPC during the penetration of the housing or its deformation. However, there is no complete physically and mathematically sound assessment of the maximum possible load that the LIPC would withstand until the onset of combustion, which covers all its physical, mechanical, and geometric indicators, the method of loading and fixing the cell.

The unifying factor of all studies is the attempt to obtain scientifically based data that could improve the safety of operation of LIPC and prevent their dangerous mechanical deformation. Improving the safety of LIPC can be possible if many factors change: the choice of steel grade of the LIPC shell, special protective equipment, etc.

In most papers, in particular [11, 12, 15], cylindrical LIPCs of format 18650 are comprehensively considered and the process of experimental research is described. However, the vast majority of studies do not consider or describe in detail the process and parameters of combustion of LIPC that should have been observed during the experiments.

The issue of physically and mathematically sound analytical determination of the maximum permissible load on the 18650 LIPC format until the occurrence of combustion remains undefined and not covered. These issues should be related to the degree and type of deformation of the LIPC body, which has its own characteristics, namely as a cylindrical shell. Also, there are almost no temperature indicators and combustion time directly due to the level of deformation damage of the Panasonic NCR18650B LIPC.

3. The aim and objectives of the study

The aim of this study is to determine the patterns of fire hazard formation in the LIPC Panasonic NCR18650B ($LiNi_{0.8}Co_{0.15}Al_{0.05}O_2$) provided its concentrated or distributed power load in terms of the danger of losing the housing stiffness reserve. Such patterns in the form of mathematical analytical dependences and experimental data would subsequently make it possible to carry out a reliable assessment of the causes and to predict the conditions for the occurrence of fires caused by LIPC of a similar format and chemical composition.

To accomplish the aim, the following tasks have been set:

– to determine the temperature indicators of LIPC during its combustion caused by mechanical deformation of its body;

– to carry out an experimental study to determine the maximum power load on LIPC until the occurrence of its combustion, subject to various options for applying the load on the LIPC housing;

– to construct a mathematical model of the process of mechanical deformation of the LIPC housing until the occurrence of obvious signs of its combustion, which will take into account the physical and mechanical properties of steel, geometric dimensions, types of deformation, and techniques of fixing the cell.

4. The study materials and methods

The main hypothesis of the study assumes that the LIPC Panasonic NCR18650B ($LiNi_{0.8}Co_{0.15}Al_{0.05}O_2$) made in Japan becomes the object of significant fire danger when its housing is mechanically deformed. Accordingly, the object of our study is the IPC Panasonic NCR18650B ($LiNi_{0.8}Co_{0.15}Al_{0.05}O_2$).

During experimental studies, the LIPC was subjected to mechanical deformation under various conditions of force application. Taking into account [7], during experimental studies, the cell was exposed exclusively to static load since it is this type of load that is used by a number of world and international standards for determining the reliability of LIPC. In addition, the application of static load makes it possible to better measure the necessary critical indicators of the cell and subsequently build a mathematical model of the process being investigated. Such experimental studies should identify and make it possible to record indicators of the fire hazard of the cell.

The laboratory bench for LIPC mechanical deformation (compression of the housing) was partially described in [17], Fig. 1.

To obtain a source of static load on the LIPC housing, a hydraulic press with a pressure gauge of 600 bar ($kg \cdot s/cm^2$) was used, manufactured in accordance with the EN 837.7 standard.

The maximum measurement error of the pressure gauge is 1 %. The use of such a hydraulic press made it possible to provide the necessary static load on the sample under study and the subsequent registration of indicators with appropriate measurement accuracy.
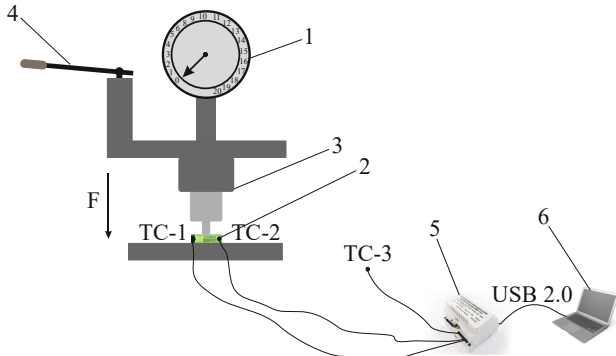

Fig. 1. Scheme of the laboratory bench for experimental research to determine the critical indicators of Panasonic NCR18650B exposed to mechanical compression:
1 — pressure gauge; 2 — Panasonic NCR18650B;
3 — hydraulic press; 4 — handle for changing the load on the hydraulic press; 5 — secondary device regulator-meter PVI—111;
6 — personal computer

Registration of temperature indicators was carried out throughout the experiment due to fixed chromel-alumel thermocouples with the possibility of registering temperature indicators from −50 to 1200 °C. Reading of indicators from thermocouples and their subsequent processing was provided by a secondary device with a regulator-meter PVI-111. One thermocouple at each of the poles was attached to the LIPC.

During the experiment, a gradual compression of the LIPC housing was carried out in increments of 11.1 bar (according to the division price) and with a delay on each division of the pressure gauge for 2–3 seconds until signs of obvious combustion appeared.

For experimental studies, 20 LIPCs were selected. All the samples studied were divided into five experimental batches, respectively, four cells in each.

tors of the fire hazard of the cell was carried out while a concentrated vertical static load was applied to the LIPC, which was placed in the horizontal plane, Fig. 2, *a*.

For point loading on the LIPC, a metal cylinder with a diameter of 20 mm was used. According to our literary review and analysis of the structure of the cell, such a mechanical load would have the most negative effect in terms of the occurrence of combustion of the cell.

During subsequent experimental studies, the LIPC housing was subjected to uniform static load on its side surface when the LIPC was placed horizontally (Fig. 2, *b*) and vertically (Fig. 2, *c*).

Conducting experimental studies using LIPC made it possible to obtain several results. In particular, in accordance with the first variant of the LLIPC load (Fig. 2, *a*), it became possible to determine the temperature indicators of the LIPC and obtain certain characteristics that make it possible to assess the level of fire hazard of LIPC Panasonic NCR18650B exposed to a static load. In particular, Fig. 3 generalizes the temperature indicators of LIPC exposed to a point static load.

In accordance with Fig. 3, it can be noted that the maximum LIPC temperature during its combustion was 580–680 °C, and the direct combustion time of the cell averages about 60–65 seconds. The above graphical dependence clearly testifies to the fact that about 30 % of the studied LIPCs may have a slightly different behavior from the total number of cells.
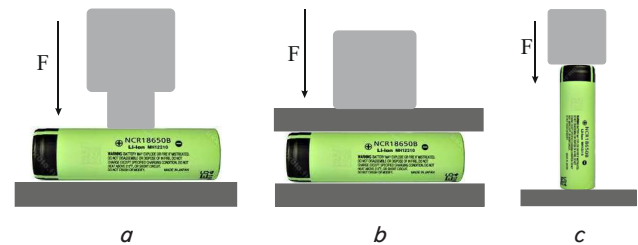

Fig. 2. Variants of applying static load to Panasonic NCR18650B during experimental studies: *a* — concentrated vertical static load on a horizontally placed cell; *b* — uniform static load on the side surface of the horizontally placed cell; *c* — vertical static load of a vertically placed cell

5. Results of studies on the determination of critical indicators of Panasonic NCR18650B exposed to static load

5. 1. Experimental establishment of temperature readings for Panasonic NCR18650B exposed to deformation of the housing

In accordance with our literary review and existing results of scientific research, several variants of deformation of the LIPC were carried out during experimental studies. First of all, the behavior of the LIPC was determined and the registration of indica-
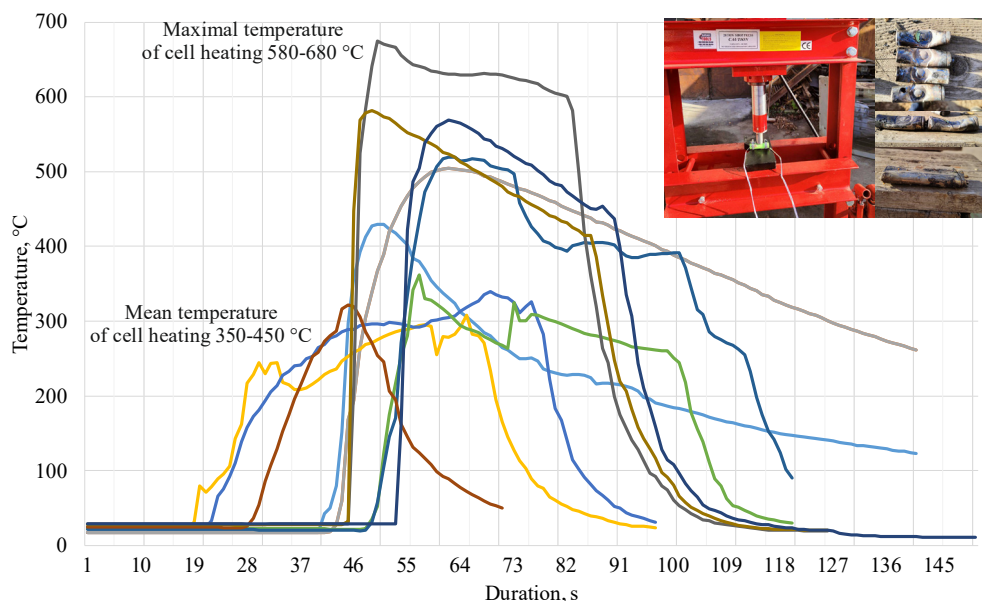

Fig. 3. Temperature indicators of Panasonic NCR18650B cells exposed to a point static load

5. 2. Experimental studies to determine the maximum power load on Panasonic NCR18650B

An important task was to determine the maximum load pressure that LIPC can withstand until the onset of its combustion. Due to the fact that the action of the concentrated static load led to the occurrence of combustion of the LIPC, it is quite natural and interesting to highlight the results of the maximum applied load, which led to the corresponding consequences (Fig. 4).

Fig. 4 shows the results of statistical processing of experimental data to determine the maximum load on the Panasonic NCR18650B cell until the occurrence of signs of its combustion. The results below (Fig. 4) indicate that the increase in the sample confirms the presence of statistical patterns and, accordingly, the expediency of mathematical modeling of the process under study and verification of the model based on experimental data.

Analysis of the magnitude of the point static load applied to the cell indicates that most studied LIPCs withstood the range of $65-85$ kg·s/cm². After that, an intensive increase in temperature indicators and the release of sparks through the poles of LIPC began. In some cases, it happened that the cell withstood a load of only $40-50$ kg·s/cm², as a result of which there was a partial destruction of the body of the cell and, ultimately, its combustion.

It should also be noted that after reaching a pressure of $90-95$ kg·s/cm², the cell self-ignited in $2-5$ seconds. This result indicates that such a load causes a chain thermochemical reaction in the cell as a result of the destruction of its inner layer and constituent cells (cathode, anode, and separator).
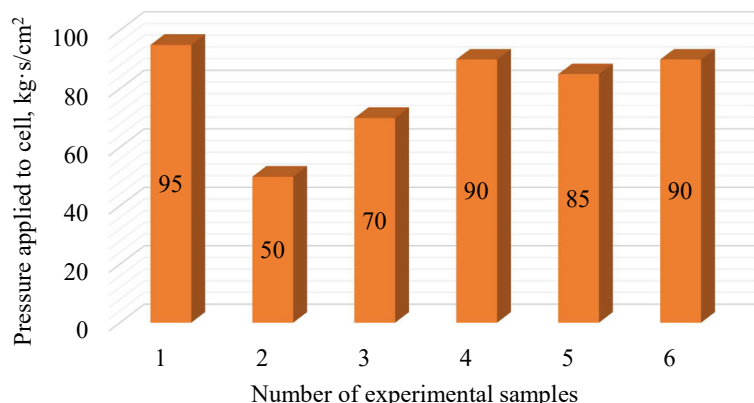

Fig. 4. Generalized histogram of the maximum load on the Panasonic NCR18650B cell until the occurrence of signs of its combustion

Summing up the results of the first series of experiments, the relative conditional deformation of the LIPC housing, until the time of combustion, at the corresponding load point was 38.5 % (110–120 mm). Accordingly, the output diameter of the cell was 180 mm (Fig. 5).

Subsequent experimental studies of the effect of static load on the LIPC, in accordance with Fig. 2, b, c, showed completely opposite results compared to the first experiment. In general, the action of the static load according to the second load scenario (Fig. 2, b) showed that all cells withstand $140-150$ kg·s/cm² (Fig. 6, a). Upon reaching the corresponding load, a short-term ignition of the LIPC occurs within 3 seconds without intensive release of sparks and flames. The temperature indicators of LIPC in this case is $300-350$ °C.

Comparing the level of deformation of the cell in Fig. 6, a with Fig. 5, it can be argued that according to the second scenario, the deformation of the LIPC was 50 % (final thickness, 90 mm) of the original diameter.

Fig. 5. Deformation of the Panasonic NCR18650B cell based on the results of exposure to a concentrated static load
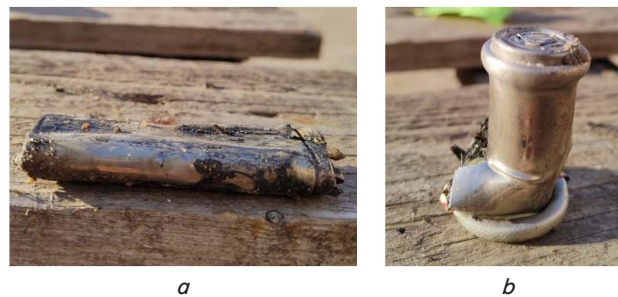

a   b

Fig. 6. Results of the static load action on the Panasonic NCR18650B cell in accordance with predefined scenarios: *a* — uniform static load on its side surface; *b* — compression of a vertically placed cell

The last scenario of the static load (Fig. 2, c), in contrast to the two previous ones, showed a completely unexpected result. In general, the deformation of the LIPC was not accompanied by combustion and an increase in temperature. The deformation and destruction of the LIPC housing occurred almost after an increase in the load from 30 kg·s/cm², after which the registration of the load indicators did not occur because the material of the LIPC housing lost its strength characteristics (Fig. 6, b).

5. 3. Mathematical modeling of the deformation process of the Panasonic NCR18650B housing caused by static point pressure

The mathematical model of the problem is considered as a circular cylindrical shell with the thickness δ, the radius R, the length l, under the action of the generalized load p_1 and p_3 in the corresponding coordinate system (Fig. 1). For the mathematical formulation of the initial ratios, the main provisions and hypotheses of the momentary theory of shells are used. Considerable attention is paid to the theoretical and experimental study of the static and dynamic mechanical behavior of cylindrical batteries, in some cases even taking into account heating, in particular [18–22], but this approach to the problem was not applied. An axisymmetric stress state arises in the shell, which is described by force factors integrated with respect to the corresponding stresses (Fig. 7). Also highlighted are the loaded cells of the median surface of the shell $d\theta\ dx$ (Fig. 8, a, b) for further integration. Accordingly, force factors are calculated.

$$N_1 = \int_{-\frac{\delta}{2}}^{\frac{\delta}{2}} \sigma_1 dz, \quad N_2 = \int_{-\frac{\delta}{2}}^{\frac{\delta}{2}} \sigma_2 dz, \tag{1}$$

$$M_2 = \int_{-\frac{\delta}{2}}^{\frac{\delta}{2}} \sigma_2 z \, dz. \tag{2}$$

The equilibrium equation is written, where the first three are identically executed:

$$\sum Y = 0, \quad \sum M_x = 0, \quad \sum M_z = 0.$$

And the rest were obtained in the form:

$$\sum X = 0, \quad \frac{dN_1}{dx} + p_1 = 0.$$

$$\sum Z = 0; \quad \frac{dQ_1}{dx} - \frac{N_2}{R} + p_3 = 0, \tag{3}$$

$$\sum M_y = 0, \quad \frac{dM_1}{dx} - Q_1 = 0.$$

After reduction by $Rd\theta dx$, infinitesimal values of higher orders are not taken into account.
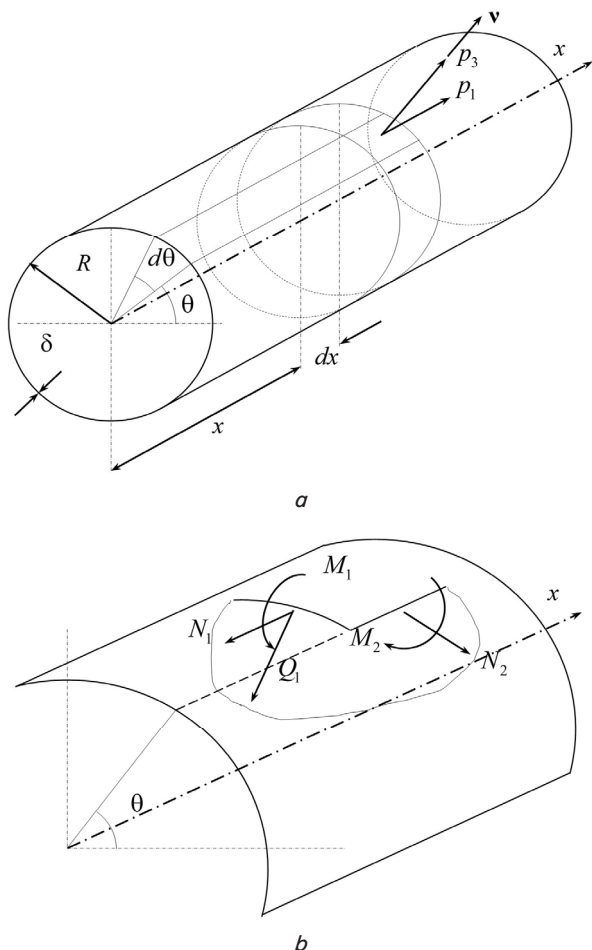

a

b

Fig. 7. General distribution of forces and moments on the power cell during calculation: a – cylindrical shell under the action of the load; b – selected side surface cell

From the first equation after its integration, we get:

$$N_1 = N_0 + \int_0^{x_1} p_1 dx, \tag{4}$$

where in most cases the load N_0 on the left side of the shell is known, and the problem of determining the forces N_1 is statically defined. The remaining two equations contain three unknown static quantities, and the problem as a whole is statically indefinite.
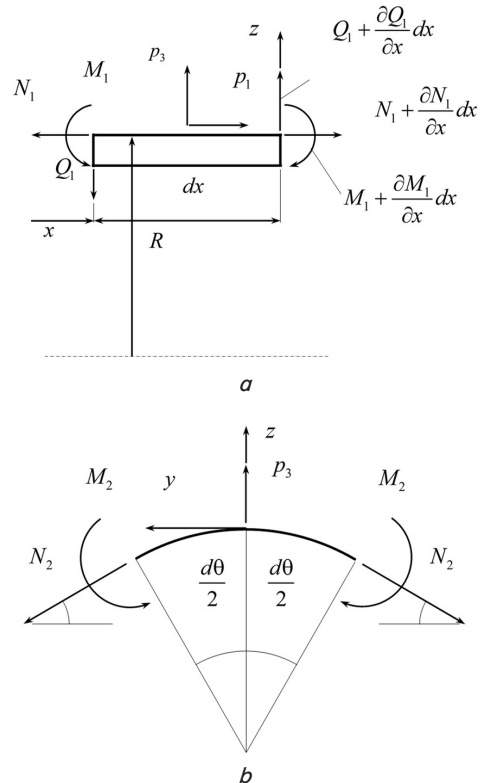

a

b

Fig. 8. Selected elements of the Panasonic NCR18650B housing for the calculation: a – selected element dx; b – selected element dθ

To solve the problem, the longitudinal movements of a point located at a distance z from the median surface are considered:

$$u(x,z) = u(x) - z\frac{dw}{dx}, \tag{5}$$

where $\frac{dw}{dx} \cong \alpha_x$ is the angle of rotation of the normal, according to a hypothesis similar to the Kirchhoff-Love hypothesis in plate theory.

Longitudinal deformation, taking into account (5), takes the form:

$$\varepsilon_1(x,z) = \frac{du(x,z)}{dx} = \frac{du}{dx} - z\frac{d^2w}{dx^2} = \varepsilon_1 + zk_1, \tag{6}$$

where ε_1 – the elongation of the median surface;

$k_1 = -\dfrac{d^2w}{dx^2}$ – the change in the curvature of the meridian in the longitudinal direction.

The deformation of the fiber, located in the circular direction at a distance z from the median surface, will be recorded:

$$\varepsilon_2 = \frac{2\pi(R+z+w) - 2\pi(R+z)}{2\pi(R+z)} = \frac{w}{R+z}. \tag{7}$$

It is taken into account here that $\cos\alpha_z \cong 1$. If we also consider that the thickness is small compared to the radius ($z \leq R$), then:

$$\varepsilon_2 = \frac{w}{R}. \tag{8}$$

We use the dependences of Hooke's generalized law, taking into account temperature, which will make it possible, if necessary, to take into account the temperature of the battery:

$$\sigma_1 = \frac{E}{1-\mu^2}(\varepsilon_1 + \mu\varepsilon_2) - \frac{E}{1-\mu}\alpha\,t,$$

$$\sigma_2 = \frac{E}{1-\mu^2}(\varepsilon_2 + \mu\varepsilon_1) - \frac{E}{1-\mu}\alpha t, \tag{9}$$

where temperature is an axisymmetric function $t=t(x,z)$, is the coefficient of temperature expansion.

Substituting expressions for deformations into formulas (9), stress is found:

$$\sigma_1 = \frac{E}{1-\mu}\left(\frac{du}{dx} - z\frac{d^2 w}{dx^2} + \mu\frac{w}{R}\right) - \frac{E\alpha\,t}{1-\mu},$$

$$\sigma_2 = \frac{E}{1-\mu}\left(\frac{w}{R} + \mu\frac{du}{dx} - \mu z\frac{d^2 w}{dx^2}\right) - \frac{E\alpha\,t}{1-\mu}, \tag{10}$$

where E is the modulus of elasticity, μ is the Poisson coefficient.

By introducing these dependences into expressions for efforts (1), (2), we obtained expressions for generalized forces in movements:

$$N_1 = \frac{E\delta}{1-\mu^2}\left(\frac{du}{dx} + \mu\frac{w}{R}\right) - N_t,$$

$$N_2 = \frac{E\delta}{1-\mu^2}\left(\frac{w}{R} + \mu\frac{du}{dx}\right) - N_t,$$

$$M_1 = -D\frac{d^2 w}{dx^2} - M_t,$$

$$M_2 = -\mu D\frac{d^2 w}{dx^2} - M_t.$$

Cylindrical stiffness is indicated here:

$$D = \frac{E\delta^3}{12(1-\mu^2)},$$

and temperature dependences:

$$N_t = \frac{E}{1-\mu}\int_{-\frac{\delta}{2}}^{\frac{\delta}{2}}\alpha t \mathrm{d}z,$$

$$M_t = \frac{E}{1-\mu}\int_{-\frac{\delta}{2}}^{\frac{\delta}{2}}\alpha t z \mathrm{d}z.$$

From the equilibrium equations (3), the transverse force is excluded:

$$\frac{dN_1}{dx} + p_1 = 0, \quad \frac{d^2 M_1}{dx^2} - \frac{N_2}{R} + p_3 = 0. \tag{11}$$

Substituting in (11) expressions for generalized forces in movements, we get:

$$\frac{d^2 u}{dx^2} + \frac{\mu}{R}\frac{dw}{dx} = \frac{1-\mu^2}{E\delta}\left(\frac{dN_t}{dx} - p_1\right),$$

$$\frac{\mu}{R}\frac{du}{dx} + \frac{w}{R^2} + \frac{\delta^2}{12}\frac{d^4 w}{dx^4} = \frac{1-\mu^2}{E\delta}\left(p_3 + \frac{N_t}{R} - \frac{d^2 M_t}{dx^2}\right). \tag{12}$$

When integrating this system, six arbitrary constants appear, which are determined from six boundary conditions – three at each end of the shell.

They can belong to longitudinal or transverse factors: to N_1 or u, to Q_1 or w, to M_1 or $\theta = \dfrac{dw}{dx}$, for example:

– hard pinching (Fig. 9, a):

$$u = 0, \; w = 0, \; \theta = 0;$$

– leaning free (Fig. 9, b):

$$N_1 = 0, \; w = 0, \; M_1 = 0;$$

– stationary hinged support (Fig. 9, c):

$$u = 0, \; w = 0, \; M_1 = 0;$$

– free edge (Fig. 9, d):

$$N_1 = 0, \; Q_1 = 0, \; M_1 = 0;$$

– joint of two shells (Fig. 9, e):

$$u^{(1)} = u^{(2)}, \; N_1^{(1)} = N_1^{(2)}, \; w^{(1)} = w^{(2)},$$

$$\frac{dw^{(1)}}{dx} = \frac{dw^{(2)}}{dx}, \; M_1^{(1)} = M_1^{(2)}, \; Q_1^{(1)} = Q_1^{(2)}.$$

Considering the force N_1 known from the solution to a statically defined problem, after transformations, from the second equation (12) we have:

$$\frac{d^4 w}{dx^4} + 4\beta^4 w = f(x), \tag{13}$$

where

$$\beta^4 = \frac{E\delta}{4DR^2} = \frac{3(1-\mu^2)}{R^2\delta^2}, \tag{14}$$

$$f(x) = \frac{1}{D}\left(p_3 - \frac{\mu}{R}N_1 + \frac{1-\mu}{R}N_t - \frac{d^2 M_t}{dx^2}\right). \tag{15}$$

General solution to equation (13):

$$w(x) = e^{-\beta x}(C_1\sin\beta x + C_2\cos\beta x) +$$
$$+ e^{\beta x}(C_3\sin\beta x + C_4\cos\beta x) + w^*(x), \tag{16}$$

where $w^*(x)$ is the partial solution to equation (12). For a slowly changing load, the partial solution can be taken as a deflection of a momentless shell: $w^* = w^m$.
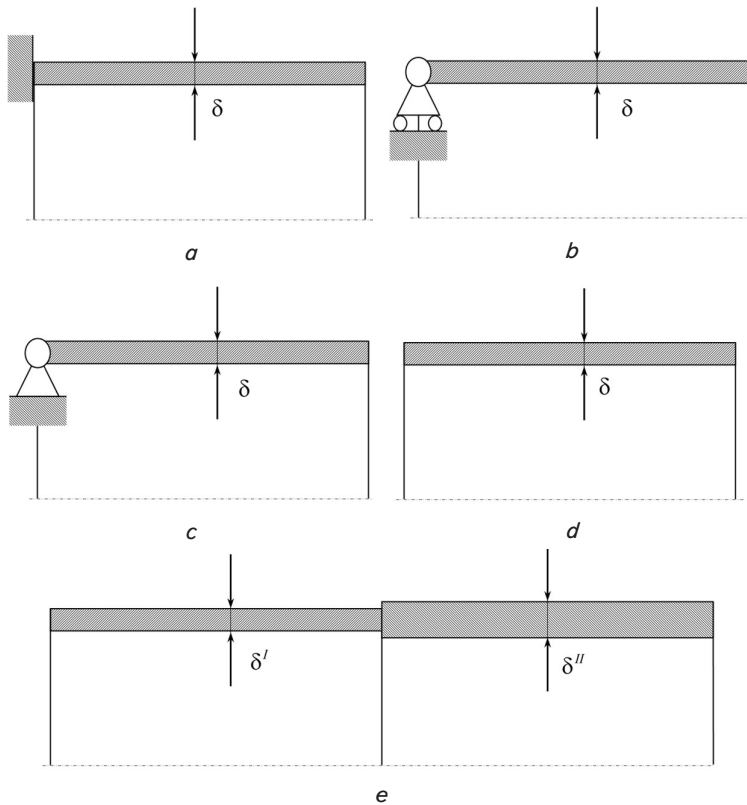
Fig. 9. Conditions for fixing the shell: *a* — hard pinching; *b* — leaning free; *c* — stationary hinge support; *d* — free edge; *e* — joint of two shells

For sufficiently long shells $l \geq 2.5\sqrt{R\delta}$ the deflection is conveniently represented in another form, where, according to the Saint-Venan principle, constants C_3, C_4 in the left end zone can be neglected.

Then:

$$w(x) = e^{-\beta x}\left(C_1 \sin\beta x + C_2 \cos\beta x\right) + w^*(x). \qquad (17)$$

Finally, according to relations (1), (2), (10), for experimental verification by ring load p, the deflection, components of moments and forces are calculated according to formulas (18) to (21). The remaining components are zero at this load while the temperature is not taken into account:

$$w = -\frac{pR^2\beta}{2E\delta} e^{-\beta x}\left(\sin\beta x + \cos\beta x\right), \qquad (18)$$

$$M_1 = \frac{-p}{4\beta} e^{-\beta x}\left(\sin\beta x + \cos\beta x\right), \qquad (19)$$

$$M_2 = \mu M_1, \qquad (20)$$

$$Q_1 = \frac{-pR\beta}{2} e^{-\beta x}\left(\sin\beta x + \cos\beta x\right). \qquad (21)$$

Using numerical analysis, the Mathcad 15 software system was used to find the relative values of the maximum values for the forces $\max w \approx 711.4\, p/E$, $\max M_1 \approx 20.3\, pE$, $\max Q_1 \approx 6.87\, p$, (modulo), where the shell dimensions of the battery are $2r = 1.82\cdot 10^{-2}$ m, $\delta = 1.25\cdot 10^{-4}$ m, with the fixation technique indicated in Fig. 5, *d*. Non-magnetic austenitic sheet steel was selected as the material of the shell (battery),

according to the national standards AISI 321, S32100 (USA), SUS321 (Japan).

Physical and mechanical characteristics for calculations are selected at a temperature of 20 °C [18–20]: modulus of elasticity, E=200 Gpa; Poisson coefficient, μ=0.3; one percent yield strength, $\sigma_y \approx$300 MPa (if necessary, here you can take into account the influence of temperature).

Comparison for the one percent yield strength of theoretical calculations according to formula (19) for maximum values with experimental data (Fig. 4) with an external load of 5 MPa showed a relative error of not more than 15 %. Obtaining such an error value is quite satisfactory, especially taking into account the statistical nature of the experimental data. Given that the ignition of LIPC corresponds to a load above 7.84 MPa, it can be assumed that the danger of ignition occurs when the load increases by more than 1.5 times. On the other hand, reaching the one percent yield strength of the battery shell material can be considered a sign of its loss of operational properties.

6. Discussion of results of investigating the effect of static load on Panasonic NCR18650B ($LiNi_{0.8}Co_{0.15}Al_{0.05}O_2$)

A complete analysis of the results of experimental studies to determine the assessment of the effect of mechanical deformation of the LIPC Panasonic NCR18650B housing showed that the place and type of applied force greatly affects its fire hazard. Thus, the concentrated static vertical load on the horizontally placed element (Fig. 2, *a*) causes the destruction of the LIPC shell. The corresponding load causes a thermochemical reaction with intensive release of sparks and an increase in the temperature of the cell to 680 °C. At the same time, the maximum allowable pressure on the LIPC at the time of combustion is 80 kg·s/ cm 2 (or 7.84 MPa) with no visible signs of combustion and temperature rise. All other types of load on the cell under consideration (Fig. 2, *b*, *c*), in general, can be attributed to those characterized by a short-term increase in temperature indicators and a short thermochemical reaction. Thus, the maximum load pressure on the cell increases to 140 kg·s/cm^2 and a relatively low temperature of 300 °C to 1 second (Fig. 6, *a*). And even, in general, the absence of signs of combustion and temperature increase as in the case of vertical static load on a vertically placed LIPC (Fig. 6, *b*). It should be noted that this type of damage to the LIPC, unlike other options [3, 4], is relatively safe in terms of fire danger. In general, the mechanical deformation of the LIPC housing is characterized by a lower heating temperature of the cell itself, lack of open combustion, and a small number of sparks.

Our experimental results that are shown in Fig. 3, 4, in contrast to [11, 12, 14, 15], fully determine the critically permissible load on LIPC until signs of combustion are detected. In particular, they make it possible to assess the temperature indicators and the nature of combustion of LIPC Panasonic NCR18650B. It should be noted that earlier studies [21–24] also did not aim to determine precisely the parameters of fire hazard of LIPC exposed to mechanical deformation.

Despite the relatively small measurement error, the disadvantage of the study is the use of metrological equipment, which allows the presence of a human factor during the acquisition and analysis of relevant indicators. In future studies of this nature, it is necessary to use measuring equipment that would make it possible to acquire research indicators automatically, which can be achieved through the use of appropriate software.

The mathematical model built has a physical and mathematical justification according to the requirements of the theory of thin shells. The effectiveness of this approach is confirmed by a satisfactory correlation with experimental data until the yield strength is reached, while the error decreases as the stresses decrease from 15 % to 7 %.

The mathematical model has limitations in application, namely the loss of shell stability. That is why there is no absolute correlation with respect to the complete data of the experimental studies carried out, in which the LIPC was deformed even after the loss of stability of the shell. The highest calculated accuracy of the model is usually achieved within the elastic stresses associated with deformations according to the linear law. Theoretical calculation shows that an increase in temperature in the range of up to 100 °C does not significantly affect the rigidity of LIPC.

The change in other geometric characteristics was not considered, due to the need to comply with standard dimensions. You can increase the rigidity by changing the steel grade, but other additional studies are needed here, for example, electrochemical effects on corrosion. Special additional LIPC fastening schemes can also increase rigidity but this requires changing the structures of their fastening. The proposed theoretical method further makes it possible, in the calculated quantitative indicators, to increase the deformation operational properties (shell rigidity) of the battery and, accordingly, the fire safety of the LIPC itself. The corresponding statement can be ensured by selecting the appropriate steel grades according to their physical and mechanical characteristics: the modulus of elasticity, the Poisson coefficient, or an increase in the thickness of the shell. In the absence of such opportunities, one has to change, namely, calculate and choose the best way to fix the battery. In further scientific research, it is necessary to focus on another type of load, in particular dynamic since it is this type of load and its impact on the fire hazard of LIPC that remains insufficiently investigated.

7. Conclusions

1. The average temperature of the cell during combustion caused by the deformation of the housing is 350–450 °C and the maximum value is registered in the range of 580–680 °C (point static load). Temperature indicators under the condition of horizontally placed LIPC and the action of a uniform static load on it on the side surface amounted to 300–350 °C. Vertical static load on the vertically placed LIPC showed no signs of combustion and a critical increase in the internal temperature of the cell.

2. Our results of experimental studies showed that, on average, the housing of the Panasonic NCR18650B LIPC can withstand a load of about 80 kg·s/cm^2 without further ignition. An increase in pressure force in the range of more than 85–90 kg·s/cm^2 leads to an irreversible chain thermochemical reaction, which within 2–3 seconds leads to the occurrence of combustion of LIPC.

3. The resulting mathematical model is structurally built on equilibrium equations for thin cylindrical shells and the ratios between stresses and deformations of Hooke's generalized law; the integration after transformations of differential equilibrium equations made it possible to write down analytical expressions to calculate permissible deformations and loads for reasons of fire danger. In contrast to the results of numerical modeling [10–16], our analytical expressions made it possible to explicitly take into account the influence of the geometric dimensions of the cylindrical shell of LIPC and the physical and mechanical characteristics of its material on the deformation resistance. The mathematical relations of the model take into account the thickness of the shell, radius and length, temperature, modulus of elasticity, and Poisson coefficient, coefficient of temperature expansion, type and magnitude of external load and the LIPC fixation technique. For example, the calculations have shown that as a result of its application, it is possible to recommend an improvement in stiffness, namely the limit of the permissible load until the steel yield is reached by 15–20 % by increasing the thickness of the shell by 10 %.

In the theoretical and experimental studies, a degree of charge of 90–100 % was adopted and the model does not take into account the influence of a lower degree of charge of the LIPC, but there is evidence [12] that the degree of charge can affect the fire hazard. That is, when using a model at low degrees of charge, one should expect a slightly overestimated assessment of fire danger.

Conflicts of interest

The authors declare that they have no conflicts of interest in relation to the current study, including financial, personal, authorship, or any other, that could affect the study and the results reported in this paper.

Funding

Data availability

All data are available in the main text of the manuscript.

References

1. Cai, Y., Ku, L., Wang, L., Ma, Y., Zheng, H., Xu, W. et al. (2019). Engineering oxygen vacancies in hierarchically Li-rich layered oxide porous microspheres for high-rate lithium ion battery cathode. Science China Materials, 62 (10), 1374–1384. doi: https://doi.org/10.1007/s40843-019-9456-1

2. Chen, X., Li, H., Yan, Z., Cheng, F., Chen, J. (2019). Structure design and mechanism analysis of silicon anode for lithium-ion batteries. Science China Materials, 62 (11), 1515–1536. doi: https://doi.org/10.1007/s40843-019-9464-0

3. Lazarenko, O., Berezhanskyi, T., Pospolitak, V., Pazen, O. (2022). Experimental evaluation of the influence of excessive electric current on the fire hazard of lithium-ion power cell. Eastern-European Journal of Enterprise Technologies, 4 (10 (118)), 67–75. doi: https://doi.org/10.15587/1729-4061.2022.263001

4. Lazarenko, O. V., Pazen, O. Y., Sukach, R. Y., Pospolitak, V. I. (2022). Experimental evaluation of fire hazard of lithium-ion battery during its mechanical damage. Naukovyi Visnyk Natsionalnoho Hirnychoho Universytetu, 5, 68–73. doi: https://doi.org/10.33271/nvngu/2022-5/068

5. Chen, Y., Kang, Y., Zhao, Y., Wang, L., Liu, J., Li, Y. et al. (2021). A review of lithium-ion battery safety concerns: The issues, strategies, and testing standards. Journal of Energy Chemistry, 59, 83–99. doi: https://doi.org/10.1016/j.jechem.2020.10.017

6. GB/T 31485-2015. Safety requirements and test methods for traction battery of electric vehicle (English Version). Available at: https://www.codeofchina.com/standard/GBT31485-2015.html

7. Ruiz, V., Pfrang, A., Kriston, A., Omar, N., Van den Bossche, P., Boon-Brett, L. (2018). A review of international abuse testing standards and regulations for lithium ion batteries in electric and hybrid electric vehicles. Renewable and Sustainable Energy Reviews, 81, 1427–1452. doi: https://doi.org/10.1016/j.rser.2017.05.195

8. Xi, S., Chang, L., Chen, W., Zhao, Q., Guo, Y., Cai, Z. (2021). Mechanical Response Analysis of Battery Modules Under Mechanical Load: Experimental Investigation and Simulation Analysis. Energy Technology, 10 (3), 2100763. doi: https://doi.org/10.1002/ente.202100763

9. Kermani, G., Keshavarzi, M. M., Sahraei, E. (2021). Deformation of lithium-ion batteries under axial loading: Analytical model and Representative Volume Element. Energy Reports, 7, 2849–2861. doi: https://doi.org/10.1016/j.egyr.2021.05.015

10. Yuan, Q., Chen, X., Meng, K., Wang, P., Tang, L., Wang, T. et al. (2022). Research on Mechanical Simulation Model and Working Safety Boundary of Large-Capacity Prismatic Lithium-Ion Battery Based on Experiment. Journal of Electrochemical Energy Conversion and Storage, 19 (3). doi: https://doi.org/10.1115/1.4054062

11. Wang, L., Yin, S., Yu, Z., Wang, Y., Yu, T. X., Zhao, J. et al. (2018). Unlocking the significant role of shell material for lithium-ion battery safety. Materials & Design, 160, 601–610. doi: https://doi.org/10.1016/j.matdes.2018.10.002

12. Xi, S., Zhao, Q., Chang, L., Huang, X., Cai, Z. (2020). The dynamic failure mechanism of a lithium-ion battery at different impact velocity. Engineering Failure Analysis, 116, 104747. doi: https://doi.org/10.1016/j.engfailanal.2020.104747

13. Xing, B., Xiao, F., Korogi, Y., Ishimaru, T., Xia, Y. (2021). Direction-dependent mechanical-electrical-thermal responses of large-format prismatic Li-ion battery under mechanical abuse. Journal of Energy Storage, 43, 103270. doi: https://doi.org/10.1016/j.est.2021.103270

14. Perea, A., Paolella, A., Dubé, J., Champagne, D., Mauger, A., Zaghib, K. (2018). State of charge influence on thermal reactions and abuse tests in commercial lithium-ion cells. Journal of Power Sources, 399, 392–397. doi: https://doi.org/10.1016/j.jpowsour.2018.07.112

15. Muresanu, A. D., Dudescu, M. C. (2022). Numerical and Experimental Evaluation of a Battery Cell under Impact Load. Batteries, 8 (5), 48. doi: https://doi.org/10.3390/batteries8050048

16. Yin, H., Ma, S., Li, H., Wen, G., Santhanagopalan, S., Zhang, C. (2021). Modeling strategy for progressive failure prediction in lithium-ion batteries under mechanical abuse. ETransportation, 7, 100098. doi: https://doi.org/10.1016/j.etran.2020.100098

17. Lazarenko, O., Pospolitak, V. (2021). Methods of testing lithium-ion batteries for fire hazard. Fire Safety, 39, 49–55. doi: https://doi.org/10.32447/20786662.39.2021.06

18. Sheikh, M., Elmarakbi, M., Rehman, S., Elmarakbi, A. (2021). Internal Short Circuit Analysis of Cylindrical Lithium-Ion Cells Due to Structural Failure. Journal of The Electrochemical Society, 168(3), 030526. doi: https://doi.org/10.1149/1945-7111/abec54

19. Zhang, X., Wierzbicki, T. (2015). Characterization of plasticity and fracture of shell casing of lithium-ion cylindrical battery. Journal of Power Sources, 280, 47–56. doi: https://doi.org/10.1016/j.jpowsour.2015.01.077

20. Material No.: AISI 321. Available at: https://woite-edelstahl.com/aisi321en.html

21. Xia, Y., Wierzbicki, T., Sahraei, E., Zhang, X. (2014). Damage of cells and battery packs due to ground impact. Journal of Power Sources, 267, 78–97. doi: https://doi.org/10.1016/j.jpowsour.2014.05.078

22. Kisters, T., Sahraei, E., Wierzbicki, T. (2017). Dynamic impact tests on lithium-ion cells. International Journal of Impact Engineering, 108, 205–216. doi: https://doi.org/10.1016/j.ijimpeng.2017.04.025

23. Xu, J., Liu, B., Wang, L., Shang, S. (2015). Dynamic mechanical integrity of cylindrical lithium-ion battery cell upon crushing. Engineering Failure Analysis, 53, 97–110. doi: https://doi.org/10.1016/j.engfailanal.2015.03.025

24. Xu, J., Liu, B., Wang, X., Hu, D. (2016). Computational model of 18650 lithium-ion battery with coupled strain rate and SOC dependencies. Applied Energy, 172, 180–189. doi: https://doi.org/10.1016/j.apenergy.2016.03.108